

Exclusive MSSM Higgs production at the LHC after Run I

M. TASEVSKY*

*Institute of Physics of the Academy of Sciences of the Czech Republic, 18221 Prague 8,
Czech Republic*

Abstract

We investigate the prospects for Central Exclusive Production (CEP) of MSSM Higgs bosons at the LHC using forward proton detectors proposed to be installed at 220 m and 420 m distance around ATLAS and / or CMS. We summarize the situation after the first and very successful data taking period of the LHC. The discovery of a Higgs boson and results from searches for additional MSSM Higgs bosons from both the ATLAS and CMS experiments, based on data samples each corresponding to about 25 fb^{-1} , have recently led to a proposal of new low-energy MSSM benchmark scenarios. The CEP signal cross section for the process $H/h \rightarrow b\bar{b}$ and its backgrounds are estimated in these new scenarios. We also make some comments about the experimental procedure if the proposed forward proton detectors are to be used to measure the CEP signal.

*email: Marek.Tasevsky@cern.ch

1 Introduction

The interest in the central exclusive production of new particles is still significant over the last decade [1–7]. The process is defined as $pp \rightarrow p \oplus \Phi \oplus p$ where all of the energy lost by the protons during the interaction (a few per cent) goes into the production of the central system, Φ . The final state therefore consists of a centrally produced system (e.g. dijet, heavy particle or Higgs boson) coming from a hard subprocess, two very forward protons and no other activity. The ' \oplus ' sign denotes the regions devoid of activity, often called rapidity gaps. A simultaneous detection of both forward protons and the central system opens up a window to a rich physics program covering not only exclusive but also a variety of QCD, Electroweak and beyond Standard Model (BSM) processes (see e.g. [3, 8–15]). Such measurements can put constraints on the Higgs sector of Minimal Supersymmetric SM (MSSM) and other popular BSM scenarios [16–27]. In SM the CEP of Higgs boson has been studied in [7, 8, 28–31].

CEP is especially attractive for three reasons: firstly, if the outgoing protons remain intact and scatter through small angles then, to a very good approximation, the primary di-gluon system obeys a $J_z = 0$, \mathcal{C} -even, \mathcal{P} -even selection rule [32, 33]. Here J_z is the projection of the total angular momentum along the proton beam axis. This allows therefore a clean determination of the quantum numbers of any observed resonance. Thus, in principle, only a few such events are necessary to determine the quantum numbers, since the mere observation of the process establishes that the exchanged object is in the 0^{++} state. Secondly, from precise measurements of the proton momentum losses, ξ_1 and ξ_2 , and from the fact that the process is exclusive, the mass of the central system can be measured much more precisely than from the dijet mass measured in the central detector, by the so-called missing mass method, $M^2 = \xi_1 \xi_2 s$ (s is the square of the proton-proton center-of-mass energy) which is independent of the decay mode. Thirdly, in CEP, in particularly so far elusive $b\bar{b}$ mode, the signal-to-background (S/B) ratios turn out to be close to unity, if the contribution from pile-up is not considered. This advantageous signal-to-background ratio is due to the combination of the $J_z = 0$ selection rule, the potentially excellent mass resolution, and the simplicity of the event signature in the central detector. Another important feature of forward proton tagging is the fact that it enables the strongest decay modes, namely $b\bar{b}$, $WW^{(*)}$ and $\tau\tau$ to be observed in one process. In this way, it may be possible to access the Higgs boson coupling to bottom quarks. This may be challenging in conventional search channels at LHC due to large QCD backgrounds although $h \rightarrow b\bar{b}$ is the dominant decay mode for a light SM Higgs boson. Here it should be kept in mind that access to the bottom Yukawa coupling will be crucial as an input also for the determination of Higgs couplings to other particles [34–37]. As already discussed in [18], measuring the proton transverse momentum and azimuthal angle ϕ distributions in forward proton detectors would enable us to search for a possible \mathcal{CP} -violating signal in the Higgs sector [38]. As shown in [38] the contribution caused by the \mathcal{CP} -odd term in the $gg \rightarrow H$ vertex is proportional to the triple-product correlation between the beam direction and the momenta of outgoing detected protons. In some \mathcal{CP} -violating MSSM scenarios [25, 26] an integrated counting asymmetry (based on counting events with $\phi > \pi$ and with $\phi < \pi$) can be sizable.

Studies of the Higgs boson produced in CEP used to form a core of the physics motivation for upgrade projects to install forward proton detectors at 420 m [9] and 220 m from the ATLAS (AFP project [10]) and CMS (PPS project [11]) detectors. At the moment, only

220 m stations are considered to be installed in ATLAS and CMS.

As it is well known, many models of new physics require an extended Higgs sector. The most popular extension of the SM is the MSSM [39–41], where the Higgs sector consists of five physical states (two Higgs doublets are required). At the lowest order the MSSM Higgs sector is \mathcal{CP} -conserving, containing two \mathcal{CP} -even bosons, the lighter h and the heavier H , a \mathcal{CP} -odd boson, A , and the charged bosons H^\pm . It can be specified in terms of the gauge couplings, the ratio of the two vacuum expectation values, $\tan\beta \equiv v_2/v_1$, and the mass of the A boson, M_A . The Higgs sector of the MSSM is affected by large higher-order corrections (see for example [42–45] for reviews), which have to be taken into account for reliable phenomenological predictions.

A brief summary of what has been studied and published in previous texts regarding the prospects of the CEP processes is given below. In [17] and [18] the CEP of the Higgs boson in MSSM at the LHC energies was studied in great detail. In [17] the detailed description is given of how the signal and all relevant background processes to all three decay modes are calculated. We plotted the enhancement factors of MSSM/SM cross sections and statistical significances in the $(M_A, \tan\beta)$ planes together with the LEP exclusion regions for the small α_{eff} scenario in the case of the WW decay and for the M_h^{max} and nomixing scenarios, defined in [46], in the case of the $b\bar{b}$ and $\tau\tau$ decays. In [18] the results in the M_h^{max} and nomixing scenarios were updated following the development on both the theory and experimental procedure side. On the theory side we have taken more accurate calculations of the process associated with bottom-mass terms in the Born amplitude contributing to the total background of the $b\bar{b}$ mode [47, 48] and used an improved version of the code **FeynHiggs** [49–53] employed for the cross section and decay width calculations. The development on the experimental side was reflected by adding the Tevatron MSSM exclusion regions corresponding to Tevatron searches for MSSM Higgs bosons. The exclusion regions were evaluated with **HiggsBounds** [54, 55]. Besides the M_h^{max} and nomixing scenarios other scenarios have been investigated, namely those yielding the correct amount of the cold dark matter abundance, the so called Cold Dark Matter (CDM) scenarios (see [56, 57] for more details), and in addition in one model beyond SM, the so called SM4 model (see e.g. [58]) with a fourth generation of quarks and leptons. While the SM4 model is practically ruled out [?] by the recent LHC measurements of Higgs-mediated cross sections [60, 61] and direct searches [62, 63], the CDM scenarios are still viable. In [18] we also stressed the importance and advantages of the CEP process in the determination of spin-parity quantum numbers of Higgs bosons.

The motivation and organization of this text is the following. Last year, the discovery of a new resonance with mass close to 125.5 GeV has been announced by the ATLAS [65] and CMS [66] experiments. Preliminary estimates of the spin-parity (by ATLAS [67], CMS [68] and Tevatron [64]) of this resonance and its couplings (by ATLAS [69] and CMS [70]) suggest that it is a Higgs boson with properties similar to the SM Higgs boson. Proving, however, that it is the Higgs boson coming exclusively from the SM, MSSM or other BSM theories will require measuring precisely its spin, \mathcal{CP} properties, mass, width and couplings which is a program for the next decade or so. At the same time, results from numerous analyses searching for the MSSM signal at LHC have been published and further analysed. Based on these results i) new low-energy MSSM benchmark scenarios have been proposed [37, 71] that are compatible over large parts of the $(M_A, \tan\beta)$ parameter plane with the mass and production rates of the observed Higgs boson signal at 125.5 GeV, and ii) the most

recent LHC exclusion regions have been evaluated using the latest version of the program `HiggsBounds` [54, 55]. The aim of this analysis is to investigate the CEP of Higgs boson in these new benchmark scenarios taking into account the recent LHC exclusion regions and the region of the allowed Higgs mass.

Luminosity scenarios

Where relevant, i.e. in benchmark scenarios where the statistical significances and signal event yields are sufficiently large, we consider two scenarios for integrated luminosity and experimental conditions for CEP processes at the LHC. As explained for example in [17, 21, 23], one of the two luminosity scenarios is to show a physics gain that could be expected if event rates are higher by a factor of 2 (due to improvements on the experimental procedure side and possibly higher signal rates), denoted by “eff×2”. We furthermore assume for sake of simplicity a center-of-mass energy of $\sqrt{s} = 14$ TeV at the LHC. Lower energies and correspondingly lower cross sections would require correspondingly higher luminosities.

- 600 fb⁻¹:

An integrated LHC luminosity of $\mathcal{L} = 2 \times 300 \text{ fb}^{-1}$, corresponding roughly to three years of running at an instantaneous luminosity $\mathcal{L} \approx 10^{34} \text{ cm}^{-2} \text{ s}^{-1}$ by both ATLAS and CMS.

- 600 fb⁻¹ eff×2:

The same integrated LHC luminosity as in the scenario with $\mathcal{L} = 2 \times 300 \text{ fb}^{-1}$ but with event rates that are higher by a factor of 2 (see the discussion of possible improvements and theoretical uncertainties in [17]).

2 Update of the MSSM analysis

A detailed description of the procedure to obtain predictions of the signal and background cross sections for all three Higgs boson decay modes is given in [17]. Their update can be found in [18]. The results shown here differ from [17, 18] mainly in the choice of MSSM benchmark scenarios and by adding the LHC exclusion regions and the allowed Higgs mass region. The formulas to calculate the signal and backgrounds in SM are the same as used in [18] (see the discussion below). Predictions within `FeynHiggs` have been updated (from the version 2.7.1 used in [18] to the version 2.9.4 used here) but the changes in `FeynHiggs` had practically no impact on our analysis. We have as well updated the `HiggsBounds` program (from the version 1.2.0 used in [18] to the version 4.0.0 used here) which is used to evaluate the LHC MSSM exclusion regions - they supersede the Tevatron exclusion regions used in [18].

Calculation of signal and $b\bar{b}$ background

The signal cross section is calculated on the basis of the prediction for the CEP of a SM Higgs boson together with an appropriate rescaling using the partial widths of the neutral

\mathcal{CP} -even Higgs bosons of the MSSM into gluons, $\Gamma(\phi \rightarrow gg)$ ($\phi = h, H$), as implemented in `FeynHiggs` (details are given in [17]).

Since the publication of [17] there was a fair development in the calculations of the CEP cross sections concerning both, the hard matrix element (see [4, 72–76]) and the so-called soft absorptive corrections and soft-hard factorization breaking effects (see [77, 78] for details and references). As discussed in [7] recent calculations of the combined enhanced and eikonal soft survival factor give lower values than the value 0.03 we used in [17]. Also taking a more appropriate factorization scale M (rather than $\approx 0.62M$) in calculating Sudakov suppression almost halves the CEP cross section (of both, the signal and background) [73]. On the other hand as discussed in [79, 80] we may expect the cross section to be increased by higher order corrections and by using the CTEQ6L [81] LO proton PDF that give the best agreement of the CEP calculations with CDF data on the exclusive $\gamma\gamma$ production [82]. A combined effect of all changes is estimated to be rather small. With the current theory accuracy of a factor of ~ 2.5 , we therefore do not feel the necessity to revise the procedure to calculate the exclusive gg -luminosity, which determines the rates of signal and background events as used in [17]. Ways to test the theoretical formalism at LHC, with or without forward proton tagging, are summarised in [83].

As explained in [18] we use the improved background formula where the NLO corrections to the bottom-mass terms in the Born amplitude were added following the results of [47]. For the term associated with the prolific $gg^{PP} \rightarrow gg$ subprocess which can mimic $b\bar{b}$ production due to the misidentification of the gluons as b jets, we still use $P_{g/b} = 1.3\%$ where $P_{g/b}$ is the probability to misidentify a gluon as a b -jet for a b -tagging efficiency of 60%.

As discussed in detail in [17], for background calculations, we use only an approximate formula. A more realistic approach is to implement all the background processes in a Monte Carlo program and to perform an analysis at the detector level (as it was done for the signal process). However none of the background processes mentioned in [17] has been implemented in any Monte Carlo event generator so far.

At luminosities greater than a few $10^{33} \text{ cm}^{-2}\text{s}^{-1}$, high-energy interactions will be accompanied by a non-negligible amount of soft interactions, so called pile-up events. The most dangerous combination arises from an overlap of the Non-diffractive dijet event with two additional Single diffraction events each having a leading proton inside the acceptance of forward detectors. The overlap of these three events can resemble a signal event and is the most prominent source of background in the $b\bar{b}$ channel at high luminosity, see [8, 9, 17, 19, 29] for details. As established in [19, 29, 84, 85] we can expect that this overlap background can be brought under control by using dedicated fast-timing proton detectors with a few pico-second resolution (see [9]) and additional experimental cuts based on the exclusivity of the event.

We emphasize that the signal selection and background rejection cuts as used for this analysis (more details about these cuts are given in the CMS-Totem document [8], while trigger strategies and optimal mass windows are explained in [17]) were chosen such that they lead to an optimal compromise between the signal yield and background reduction. It is important to mention that the signal and background yields from that CMS study are in a fair agreement with those reported in two ATLAS analyses [19, 29] which both operated at one mass point, $M_h = 120 \text{ GeV}$. As explained in [17], the overlap background cross section is huge and therefore the background rejection cuts are very stringent which leads also to a significant reduction of the signal. The remaining background is not zero

but similarly to [17] and [18], we anticipate improvements in the experimental procedure, for example smaller misidentification probability $P_{g/b}$ (cf. the improvement in the light-quark-b misidentification, $P_{q/b}$, techniques in ATLAS [86] and in CMS [87]), multivariate techniques or better resolution in timing detectors which can reduce the overlap backgrounds down to a negligible level. Hence the pile-up effects are assumed to be negligible after applying all the cuts suppressing the pile-up.

New benchmark scenarios

Due to the large number of MSSM parameters, a number of benchmark scenarios [46,88] have usually been used for the interpretation of MSSM Higgs boson searches at LEP [89], Tevatron [90] and LHC [91], such as M_h^{\max} , no-mixing, small α_{eff} and gluo-phobic Higgs scenarios. The M_h^{\max} , no-mixing and small α_{eff} scenarios have been used to evaluate our first results [17]. Their updates have been published in [18] where also more general benchmark scenarios have been examined, the so called CDM scenarios (explained in the previous section).

In this paper we investigate prospects for the CEP of Higgs boson in the new benchmark scenarios that have been proposed recently in [71]. Here we briefly summarize their main features, while their detailed description can be found in [71].

1. The M_h^{\max} scenario:

Mass of the lightest \mathcal{CP} -even Higgs boson is maximised at large M_A for a given $\tan\beta$. A slight modification compared to the standard M_h^{\max} scenario is an increase of the gluino mass from 0.8 TeV to 1.5 TeV which follows limits from direct searches for SUSY particles at LHC [92]. In this scenario M_h is in agreement with the discovery of a Higgs-like state only in a relatively narrow strip at rather low $\tan\beta$.

2. The Mhmod+ scenario:

The M_h^{\max} scenario can be modified such that in the decoupling regime the M_h values are close to the observed mass of the Higgs signal over a wide region of parameter space. The modification consists of reducing the amount of mixing in the stop sector, i.e. reducing $|X_t/M_{\text{SUSY}}|$ (M_{SUSY} is the mass of stop and sbottom) compared to a value of ≈ 2 used in the M_h^{\max} scenario (Feynman-diagrammatic calculation). This can be done for both signs of X_t . In this scenario this ratio is reduced to 1.5.

3. The Mhmod- scenario:

Similarly as for the Mhmod+ scenario but with negative X_t , $X_t/M_{\text{SUSY}} = -1.9$.

4. The Light stop scenario:

This scenario can be regarded as an update of the gluo-phobic scenario used in the past. Values of X_t in the range $2M_{\text{SUSY}} < X_t < 2.5M_{\text{SUSY}}$ lead to reduced gluon fusion rates. In this scenario $X_t = 2M_{\text{SUSY}}$ and $M_{\text{SUSY}} = 500$ GeV. Such a large value of $|X_t|$ and a relatively low value of M_{SUSY} necessarily lead to the presence of a light stop.

5. The Light stau scenario:

The motivation for this scenario stems from the measured diphoton rate of the discovered Higgs boson that is somewhat larger than the expectations for a SM Higgs. Such an enhanced diphoton rate of the lightest \mathcal{CP} -even Higgs boson may be achieved in a scenario with light staus if a sufficiently large stau mixing, X_τ , is present.

6. The Tau-phobic Higgs scenario:

This scenario can be regarded as an update of the small α_{eff} scenario used in the past. Thanks to propagator-type corrections involving the mixing between the two \mathcal{CP} -even Higgs bosons of MSSM the Higgs coupling to down-type fermions can be significantly modified which can approximately be termed via an effective mixing angle α_{eff} . This modification occurs for large values of $A_{t,b,\tau}$ parameters (denoting Higgs-stop, Higgs-sbottom coupling and soft SUSY-breaking parameter in the scalar tau sector, respectively) and large values of μ (higgsino mass parameter) and $\tan \beta$.

7. The Low-MH scenario:

In this scenario the observed Higgs boson at 125.5 GeV is identified with the heavy Higgs boson of the MSSM and behaves roughly SM-like. In this case the Higgs sector is very different from the SM one because all five MSSM Higgs bosons would be light. The light \mathcal{CP} -even Higgs boson of the MSSM would have heavily suppressed couplings to gauge bosons. In this scenario a low value of M_A is required and therefore there is no point in varying M_A . It is thus fixed to the value of 110 GeV and the μ is varied instead. We have checked that other low values of M_A do not affect the final conclusions. The remaining parameters are chosen the same as in the Tau-phobic Higgs scenario, with the exception of setting $M_{l3} = 1000$ GeV (denoting soft SUSY-breaking parameter in the scalar neutrino sector), while in the Tau-phobic Higgs is $M_{l3} = 500$ GeV. Note that very recent ATLAS results [93] setting exclusion limits on the mass of light charged Higgs boson are not yet considered here. They may result in a further enlargement of the existing exclusion regions for this scenario but a dedicated analysis of those bounds in this scenario is still necessary to be carried out.

We remind that in the scenarios 1–6 the discovered Higgs boson is the \mathcal{CP} -even lightest Higgs boson and we are looking for its heavier partner, while in the scenario 7 the situation is opposite.

Bounds from Higgs searches at LEP and the LHC

Higgs bosons of the SM and the MSSM have been searched for at LEP [89, 94], Tevatron [64, 90] and LHC [67–70, 91]. In our first paper [17] results were shown in $(M_A, \tan \beta)$ planes with regions excluded by MSSM Higgs searches at LEP. In the second paper [18] the exclusion regions coming from Tevatron MSSM Higgs searches were added. In this analysis the Tevatron MSSM exclusion regions are superseded by the LHC MSSM exclusion regions. They correspond to results from direct searches for MSSM Higgs bosons at LHC. The search is pursued mainly via the channels $(\Phi = h, H, A)$:

- $pp \rightarrow \Phi \rightarrow \tau^+ \tau^-$ (inclusive);
- $b\bar{b}\Phi, \Phi \rightarrow \tau^+ \tau^-$ or $b\bar{b}$ (with b -tag);
- $pp \rightarrow t\bar{t} \rightarrow H^\pm W^\mp b\bar{b}, H^\pm \rightarrow \tau \nu_\tau$;
- $gb \rightarrow H^- t$ or $g\bar{b} \rightarrow H^+ \bar{t}, H^\pm \rightarrow \tau \nu_\tau$.

The $(M_A/M_{H^\pm}, \tan \beta)$ parameter space is constrained by the absence of any additional state in these production and decay modes, while the masses of the first and second generation scalar quarks and the gluino, and to a lesser degree of the stop and sbottom masses are constrained by the absence of SUSY particles (see [92] for a recent summary).

The bounds obtained at the LEP, Tevatron and LHC (with the exception of the ATLAS analysis on the charged Higgs boson [93] as described for the scenario 7) have been implemented into the Fortran code **HiggsBounds** [54, 55] (linked to **FeynHiggs** [49–53] to provide the relevant Higgs masses and couplings). The full sets of analyses used to evaluate the exclusion regions are listed in the manual to the **HiggsBounds** program [54, 55]. For any parameter point provided to **HiggsBounds** the code determines whether it is excluded at the 95% C.L. based on the published exclusion data. These excluded regions from LEP *and* the LHC are marked in the MSSM scenario plots shown below. We have used the version **HiggsBounds** 4.0.0 for our evaluations.

3 Prospects for neutral \mathcal{CP} -even Higgs bosons in the new benchmark MSSM scenarios

In this section we present the prospects for observing the neutral \mathcal{CP} -even MSSM Higgs bosons in CEP. We display our results in the $(M_A, \tan \beta)$ planes for seven benchmark scenarios recently proposed in [71] and briefly specified in the previous section. Also shown in the plots are the parameter regions excluded by the LEP Higgs searches (as dark shaded (blue) areas) and LHC Higgs-boson searches (as lighter shaded (red and eventually pink) areas) as obtained with **HiggsBounds** [54, 55]. The SM cross section used [95] for the normalization within **HiggsBounds** is evaluated using the MRST2002 NNLO PDFs [96]. The use of the updated version, namely MSTW2008 [97] results in a reduction of the cross section by $\sim 20\%$, while (as discussed in the previous section) the CTEQ6L PDFs [81] which give closest predictions to the results obtained in the exclusive $\gamma\gamma$ analysis in CDF [82] would increase the CEP Higgs cross section by a factor of almost 3. For each point in the parameter space we have evaluated the relevant Higgs production cross section times the Higgs branching ratio corresponding to the decay mode under investigation. The Higgs-boson masses, the decay branching ratios and the effective couplings for the production cross sections have been calculated with the program **FeynHiggs** [49–53]. The resulting theoretical cross section has been multiplied by the experimental efficiencies taking into account detector acceptances, experimental cuts and triggers as discussed in [17].

Where it is relevant, this procedure has been carried out for two different assumptions on the luminosity scenario, see Sect. 1, for which the contours for 3σ significances have been obtained. In remaining cases only theoretical production cross sections are evaluated and

plotted. In figures we also plot by the light gray (green) so called region of allowed Higgs masses, i.e. $M_h = 125.5 \pm 3$ GeV for scenarios 1–6 and $M_H = 125.5 \pm 3$ GeV for the Low-MH scenario. The total uncertainty of 3 GeV represents a combination of the experimental uncertainty of the measured mass value (~ 0.6 GeV) and of the theoretical uncertainty in the MSSM Higgs mass prediction from unknown higher-order corrections.

In our analysis we concentrate only on the $b\bar{b}$ decay mode. The reason is that in the parameter space not excluded by the LHC exclusion regions and combined with the region of allowed mass of the discovered Higgs boson (roughly $6 < \tan\beta < 10$ and $M_{H/h} > 250$ GeV) the final theoretical cross sections for the $\tau\tau$ decay mode are lower than those for the $b\bar{b}$ decay mode. The CEP process with subsequent decay into bottom quarks is of particular relevance since this channel may provide a unique possibility for directly accessing the $hb\bar{b}$ coupling at LHC¹ although the decay into bottom quarks is by far the dominant decay mode of the lighter \mathcal{CP} -even Higgs boson in nearly the whole parameter space of the MSSM (and it is also the dominant decay of a light SM-like Higgs). For this reason information on the bottom Yukawa coupling is important for determining *any* Higgs-boson coupling at the LHC (rather than just ratios of couplings), see [34, 35, 101].

3.1 Scenarios M_h^{\max} , Mhmod+, Mhmod-, Light stop, Light stau and Tau-phobic Higgs

In Figs. 1, 2 and 3 we show the theoretical cross sections of the $H \rightarrow b\bar{b}$ channel in CEP in the $(M_A, \tan\beta)$ plane of the MSSM within the benchmark scenarios 1 to 6. We remind that in the scenarios 1–6 the discovered Higgs boson is considered to be the lighter one, while we are looking for its heavier partner. We note that the light Higgs behaves more or less SM-like (although the ggh coupling can be lower and/or the $hb\bar{b}$ and $h\tau\tau$ couplings may be reduced somewhat), and thus the prospects for the light Higgs are effectively those of the SM one (see e.g. [102] where we have shown available cross sections for both the light and heavy MSSM Higgs bosons produced via CEP and constrained by the Higgs boson discovery and MSSM exclusion regions).

In Fig. 1 the results are shown for scenarios M_h^{\max} (left) and Tau-phobic Higgs (right), in Fig. 2 for scenarios Mhmod+ (left) and Mhmod- (right) and in Fig. 3 for scenarios Light stop (left) and Light stau (right). The values of the mass of the heavy \mathcal{CP} -even Higgs boson, M_H , are indicated by dashed (black) contour lines, while the values of the theoretical cross sections are indicated by the solid (blue) lines. The dark shaded (blue) region corresponds to the parameter region that is excluded by the LEP Higgs searches, the lighter shaded (red) areas are excluded by LHC Higgs searches. The region of the allowed Higgs mass is plotted as a lighter gray (green) band for masses $M_h = 125.5 \pm 3$ GeV.

The region of interest is the area of allowed Higgs masses that is not overlaid by the LHC exclusion region. In different scenarios it covers different phase space: for the M_h^{\max} scenario it roughly represents a band delimited by $\tan\beta$ between 4 and 10 and M_A starting at about 250 GeV. For remaining scenarios 2–6 the allowed Higgs mass region represents a wedge which starts at $(M_A, \tan\beta) = (270 \text{ GeV}, 6)$ for the Mhmod+ and Mhmod-, at (410 GeV,

¹ Another interesting idea to access the $b\bar{b}$ coupling to the Higgs boson is the production via Higgsstrahlung, $V^* \rightarrow VH$ ($V = W^\pm, Z$) in a strongly boosted system [98–100].

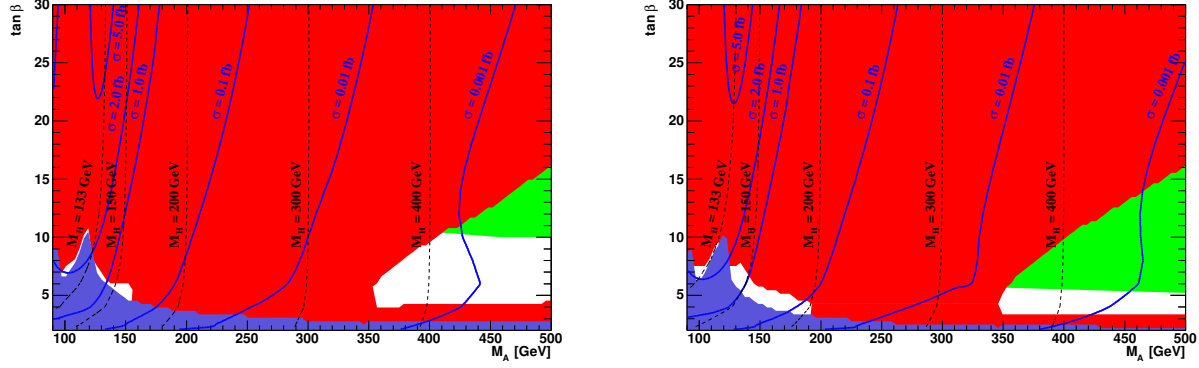


Figure 3: Contours of signal cross sections (solid blue lines) for the $H \rightarrow b\bar{b}$ channel in CEP at $\sqrt{s} = 14$ TeV in the $(M_A, \tan\beta)$ plane of the MSSM within the Light stop (left plot) and Light stau (right plot) benchmark scenario. The values of the mass of the heavy \mathcal{CP} -even Higgs boson, M_H , are indicated by dashed (black) contour lines. The dark shaded (blue) region corresponds to the parameter region that is excluded by the LEP MSSM Higgs searches, the lighter shaded (red) area is excluded by the LHC MSSM Higgs searches. The light shaded (green) area corresponds to the allowed light Higgs mass region $122.5 < M_h < 128.5$ GeV.

than 0.02 fb) to be considered seriously for further studies.

In general, the CEP of the heavier \mathcal{CP} -even Higgs boson of the MSSM with subsequent decay into bottom quarks provides a unique opportunity for accessing its bottom Yukawa coupling in a mass range where for a SM Higgs boson the decay rate into bottom quarks would be negligibly small. However, due to a massive exclusion coming from the LHC MSSM searches, the allowed region concentrates at very low $\tan\beta$ values. In this region the enhancement factors MSSM/SM are around 50 (see [102]) but the cross section for the production of the SM Higgs boson in CEP is too small.

3.2 Low-MH scenario

We now turn to the prospects for producing the \mathcal{CP} -even Higgs boson in CEP channels in the Low-MH scenario. We remind that in this scenario the discovered Higgs boson is considered to be the heavier one, while we are looking for its lighter partner. As explained in Sect. 2 the most convenient way to present results is using the $(\mu, \tan\beta)$ plane rather than the $(M_A, \tan\beta)$ plane used in the scenarios 1–6. In Figs. 4, 5 and 6 results for the cross sections, ratios of signal to background cross sections (S/B) and statistical significances are presented by solid (blue) contour lines. The values of the mass of the light \mathcal{CP} -even Higgs boson are indicated by dashed (black) contour lines. Similarly to the color coding for the scenarios 1–6, the light shaded (green) band represents the region of allowed mass of the discovered Higgs boson, in this case of the heavy one, namely $122.5 < M_H < 128.5$ GeV. The dark shaded (blue) region represents the LEP MSSM exclusion region, the lighter shaded (red), the lighter shaded (pink) and black areas are excluded by LHC MSSM Higgs searches in the analyses of $h/H/A \rightarrow \tau\tau$, charged Higgs and Higgs rates, respectively. As described in Sect. 2, the results of the ATLAS analysis on the charged Higgs bosons [93] are not included

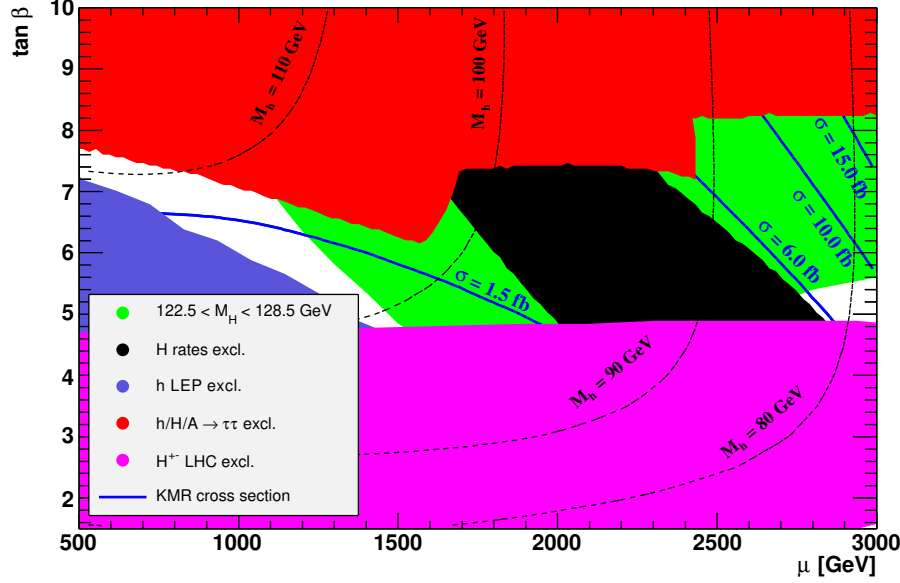


Figure 4: Contours of signal cross section (solid blue lines) for the $h \rightarrow b\bar{b}$ channel in CEP at $\sqrt{s} = 14$ TeV in the $(\mu, \tan \beta)$ plane of the MSSM within the Low-MH benchmark scenario. The values of the mass of the light \mathcal{CP} -even Higgs boson, M_h , are indicated by dashed (black) contour lines. The dark shaded (blue) region corresponds to the parameter region that is excluded by the LEP MSSM Higgs searches, the lighter shaded (red), the lighter shaded (pink) and black areas are excluded by LHC MSSM Higgs searches in the analyses of $h/H/A \rightarrow \tau\tau$, charged Higgs and Higgs rates, respectively. The light shaded (green) area corresponds to the allowed mass region $122.5 < M_H < 128.5$ GeV.

in the exclusion regions.

In Fig. 4 we show the theoretical signal cross section for the $h \rightarrow b\bar{b}$ channel in the CEP. As can be seen, the signal cross section is an increasing function of μ reaching its maximum value of about 15 fb at values close to $\mu = 3000$ GeV and mass M_h close to 80 GeV. Note that for normalization purposes at a mass of 125 GeV we take for the SM CEP cross section the value of 1.9 fb, see [7] for details.

In Fig. 5 the ratios S/B for two forward proton detector configurations, namely the total 420+220 and 420+420 (denoted by 420+220 in Fig. 5) and the 420+420 alone, are presented. The advantage of plotting this ratio is that various uncertainties (such as those connected with the soft survival factor, (N)NLO effects, choice of proton PDFs etc.) are canceled. To be closer to reality, we decided to multiply the theoretical cross sections (those plotted in Fig. 4) by the experimental efficiencies and integrate over optimal mass windows. The procedure to get the optimal mass windows from the point of view of the highest S/B ratio is described in [17].

We see that for both forward proton detector configurations, the highest S/B values are about 0.2 and they are located roughly in the same corner as the highest signal cross section region seen in Fig. 4. The region of interest is therefore $(\mu, \tan \beta) = (2500\text{--}3000 \text{ GeV}, 6\text{--}8)$,

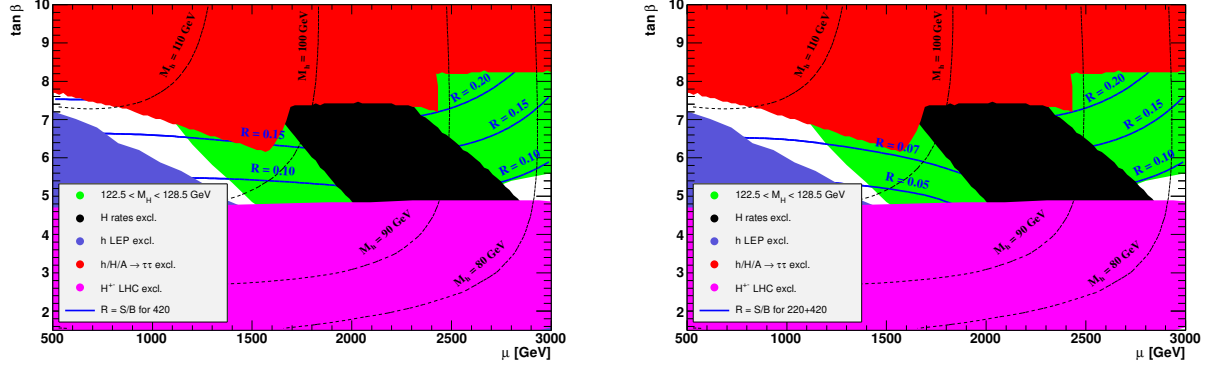


Figure 5: The ratio of signal/background cross sections (solid blue lines) for the $h \rightarrow b\bar{b}$ channel in CEP at $\sqrt{s} = 14$ TeV in the $(\mu, \tan\beta)$ plane of the MSSM within the Low-MH benchmark scenario for the 420+420 (Left plot) and the 420+220 (Right plot) forward proton detector configuration. In the evaluation of the ratio, both signal and background cross sections are multiplied by the total experimental efficiencies. The values of the mass of the light \mathcal{CP} -even Higgs boson, M_h , are indicated by dashed (black) contour lines. The dark shaded (blue) region corresponds to the parameter region that is excluded by the LEP MSSM Higgs searches, the lighter shaded (red), the lighter shaded (pink) and black areas are excluded by LHC MSSM Higgs searches in the analyses of $h/H/A \rightarrow \tau\tau$, charged Higgs and Higgs rates, respectively. The light shaded (green) area corresponds to the allowed mass region $122.5 < M_h < 128.5$ GeV.

i.e. $(\mu, M_h) = (2500\text{--}3000 \text{ GeV}, 80\text{--}90 \text{ GeV})$. In spite of the relatively high signal cross sections, the S/B ratios are only moderate. The explanation is twofold: i) theoretical cross sections for the irreducible backgrounds are steeply falling functions of mass, see formula (8) in [18] composed of mass terms of powers of -6 and -8; ii) experimental efficiencies, mass resolution and acceptances are also functions of mass, however much less steep and more importantly increasing/improving with mass. So in summary, if we move the mass of interest from the region of e.g. 120 GeV down to the region of 80–90 GeV, the background cross sections greatly increase, while the efficiencies and acceptances decrease and the mass resolution slightly worsens (see e.g. Fig. 3.7 (right) in [8]). In evaluating the S/B ratio, all these experimental effects are properly taken into account including the fact that the optimal mass windows for both the individual 420+420 and 420+220 configurations over which the signal and background are integrated enlarge with decreasing mass. When comparing these S/B ratios between the 420+420 and the total sum (i.e. Fig. 5 left and right), we see that the ratios are identical for masses lower than roughly 100 GeV, while they are higher for the 420+420 configuration for masses greater than roughly 100 GeV. This is explained by the mass acceptance of the proposed forward proton detectors: in the region $M_h < 100$ GeV, only the 420+420 configuration contributes, while in the region $100 < M_h < 120$ GeV, both configurations are important. Due to a much broader optimal mass window for the 420+220 than for the 420+420 in the latter mass range, we pick up much more background than with the 420+420 only and hence the contribution of the 420+220 configuration makes the total S/B smaller than the S/B for the 420+420 configuration alone.

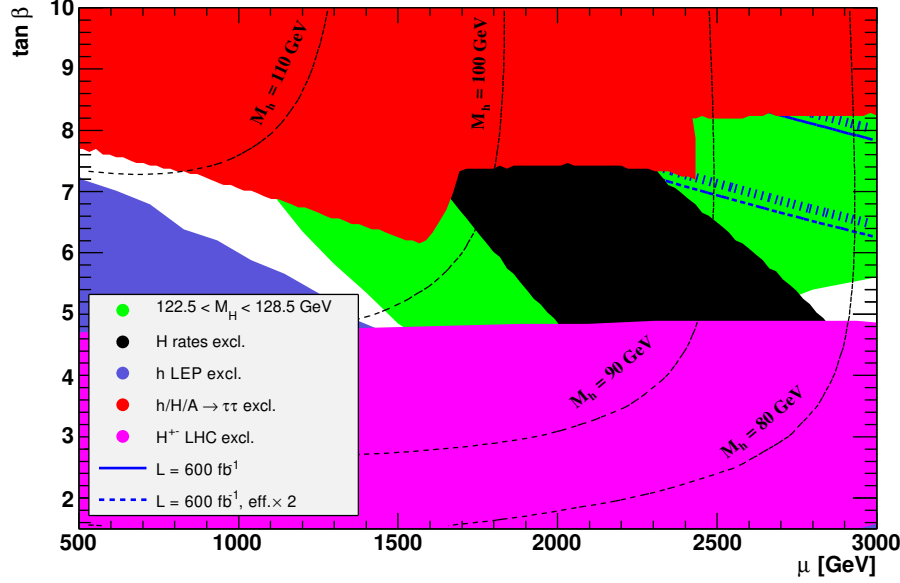


Figure 6: Contours of 3σ statistical significance (solid blue lines) for the $h \rightarrow b\bar{b}$ channel in CEP at $\sqrt{s} = 14$ TeV in the $(\mu, \tan\beta)$ plane of the MSSM within the Low-MH benchmark scenario. The results are shown for assumed effective luminosities (see text, combining ATLAS and CMS) of 600 fb^{-1} and $600 \text{ fb}^{-1} \text{ eff} \times 2$. The values of the mass of the light \mathcal{CP} -even Higgs boson, M_h , are indicated by dashed (black) contour lines. The dark shaded (blue) region corresponds to the parameter region that is excluded by the LEP MSSM Higgs searches, the lighter shaded (red), the lighter shaded (pink) and black areas are excluded by LHC MSSM Higgs searches in the analyses of $h/H/A \rightarrow \tau\tau$, charged Higgs and Higgs rates, respectively. The light shaded (green) area corresponds to the allowed mass region $122.5 < M_H < 128.5$ GeV.

In Fig. 6 we present the contours of 3σ statistical significance for the $h \rightarrow b\bar{b}$ channel in CEP for the 420+220 configuration. The results are shown for assumed effective luminosities of 600 fb^{-1} and $600 \text{ fb}^{-1} \text{ eff} \times 2$. It is not surprising that the highest achievable significances are located in the same corner of the green band as have been located the highest S/B ratios in Fig. 5 (right) plot. We also note that this 3σ statistical significance plot for the 420+420 configuration is identical to the Fig. 6 and therefore it is not shown. The reason why it is identical is straightforward: the region of interest (i.e. significances larger than 3σ) is in the area where Higgs masses are very low, namely $80 < M_h < 90$ GeV. This mass region is unreachable with the 420+220 configuration, while the mass acceptance of the 420+420 there is above 40% (see e.g. Fig. 3.7 (left) in [8]). We may conclude that if the MSSM should be realized as in the Low-MH scenario, i.e. the heavy Higgs boson to be seen at mass of 125.5 GeV and the lighter one in the range of 80–90 GeV, then forward proton detector projects could be very helpful to both ATLAS and CMS. At the moment, there are no direct searches at LHC for a Higgs boson in such a low-mass region. We emphasize that this light Higgs boson could be only seen with stations at 420 m, the less distant stations do not

contribute.

A few notes about experimental issues, however, are necessary to make at this place. First, from the Fig. 6 we see that the total integrated luminosity needed to observe the light Higgs boson produced in CEP with mass around 80–90 GeV is of the order of 1000 fb^{-1} . Current estimates of the total amount of acquired data for proposed forward proton detector projects at LHC, the AFP and PPS, for realistic data taking scenarios at instantaneous luminosities in the range of $2\text{--}10 \times 10^{32} \text{ cm}^2 \text{ s}^{-1}$ are of the order of 500 fb^{-1} . This means that to observe the light Higgs boson with forward proton detectors at this mass range, data from both the AFP and PPS would have to be combined. Furthermore, putting the AFP stations at 420 m into the L1 trigger in ATLAS trigger scheme would be hardly possible due to a shorter L1 latency than the time needed for a proton signal in AFP to be processed and sent back to the Central Trigger Processor. The ways to tackle this problem in ATLAS are for example to use existing jet and muon triggers at L1 and reducing their rates at L2 by incorporating into L2 the track and time information about protons in both 420 stations [19] or by adding an information about jet p_T , η and ϕ into the L1 calorimeter [103]. In CMS the current latency is larger than the one of ATLAS and there are plans to even enlarge it after the Long Shutdown 1. And finally, as was already mentioned, the total mass acceptance decreases and the mass resolution worsens with decreasing mass. Another quantity that also deteriorates with decreasing mass is the b-tagging efficiency. Interestingly the light-quark-b misidentification, $P_{q/b}$, improves with decreasing jet transverse energy [86, 87]. On the other hand there are areas where a further reduction of the background may be expected. We remind that we use $P_{g/b} = 1.3\%$ which is at the moment very conservative given the development seen in ATLAS [86] and CMS [87] in this area. Another area with a fair development is fast timing detectors where a sub-10 ps resolution in a near future is not excluded, if supported by a proper R&D program. We conclude that investigating the mass range of 80–90 GeV with forward proton detectors at LHC is more challenging than that around 120 GeV.

4 Conclusions

We have re-analysed in this paper the prospects for probing the Higgs sector of MSSM with central exclusive Higgs-boson production processes at the LHC, utilizing forward proton detectors proposed to be installed at 220 m and 420 m distance around ATLAS and/or CMS. The analysis has been performed for CEP of the neutral \mathcal{CP} -even Higgs bosons h and H of the MSSM and their decays into bottom quarks.

Changes with respect to previous papers [17, 18] are the following. Firstly the Tevatron MSSM exclusion regions shown in [18] have been superseded by the LHC MSSM exclusion regions extracted from the most recent compilation of the LHC MSSM Higgs boson searches. Secondly the LHC Higgs boson discovery announced last year is accounted for in figures by putting the allowed Higgs boson mass band $122.5 < M_{h/H} < 128.5 \text{ GeV}$. And thirdly the results are presented in seven new recently proposed low-energy MSSM benchmark scenarios which all are compatible with the mass and production rates of the observed Higgs boson signal at 125.5 GeV. In six scenarios, namely M_h^{max} , Mhmod+, Mhmod-, Light stop, Light stau and Tau-phobic Higgs, the discovered Higgs boson is considered to be the light \mathcal{CP} -even Higgs boson and in the usual $(M_A, \tan \beta)$ planes we investigate the predicted CEP signal of

its heavier MSSM partner in the allowed Higgs mass band. In the seventh scenario, namely the Low-MH, the discovered Higgs boson is considered to be the heavy \mathcal{CP} -even Higgs boson and we study the signal of its lighter MSSM partner in the allowed Higgs boson mass band. Results in this scenario are more convenient to present in the $(\mu, \tan\beta)$ plane. Compared to last published results in [18], the LEP and LHC exclusion regions rule out most of the MSSM parameter space. The unexcluded (but at the same time allowed by the LHC Higgs boson discovery) region concentrates into a wedge area of small $\tan\beta$, $\tan\beta < 15$ at $M_H = 500$ GeV where the $\tan\beta$ threshold decreases with decreasing value of M_H .

We find that in scenarios 1–6 the theoretical CEP signal cross sections are too small to produce a detectable signal within a reasonable time scale for making use of forward proton detectors.

The Low-MH scenario gives a much more promising sensitivity. We observe that the highest cross sections, S/B ratios and statistical significances are located in the corner $(\mu, \tan\beta) = (2500\text{--}3000 \text{ GeV}, 6\text{--}8)$, i.e. $(\mu, M_h) = (2500\text{--}3000 \text{ GeV}, 80\text{--}90 \text{ GeV})$ which is still not excluded by LHC MSSM Higgs searches (as mentioned before, the recent ATLAS results on the charged Higgs boson [93] are not included) and lies in the allowed mass range set up by the Higgs boson discovery at 125.5 GeV. We find that a light Higgs boson of mass 80–90 GeV decaying into $b\bar{b}$ and produced via CEP can be observed with 3σ significance if an integrated luminosity of around 1000 fb^{-1} is provided. Collecting such an amount of data would most likely require to combine data from both the ATLAS and CMS forward proton detectors. The low mass state of 80–90 GeV can only be detected with forward proton detectors placed at 420 m from the interaction point, less distant stations do not contribute due to zero mass acceptance in this mass region. We also comment on the challenge to detect reliably a Higgs boson candidate at such a low mass. Besides the total mass acceptance decreasing and the mass resolution worsening also the b-tagging efficiency deteriorate as mass decreases. On the other hand, we believe that there is still room for improvement of experimental techniques, let us mention e.g. the expected improvement of the gluon-b misidentification probability $P_{g/b}$ compared to the 1.3% used in our original paper, a sub-10 ps resolution in timing detectors or the use of multivariate techniques.

It may turn out that the observed Higgs boson at mass of 125.5 GeV is of the purely SM nature. Then for the CEP and forward proton detector projects to be useful to ATLAS and CMS in measuring properties of the SM Higgs boson, the S/B ratio needs to be considerably increased. All improvements mentioned above are also applicable to the mass region around 120 GeV and will certainly lead to a non-negligible increase of S/B.

A striking feature of CEP Higgs-boson remains that this channel provides a valuable information on the spin and the coupling structure of Higgs candidates at the LHC. We emphasize that the $J_z = 0$, \mathcal{C} -even, \mathcal{P} -even selection rule of the CEP process enables us to estimate very precisely (and event-by-event) the quantum numbers of any resonance produced via CEP.

Finally we remind that the proposed forward proton detectors would offer an unique possibility to probe the \mathcal{CP} -violation in the Higgs sector by measuring the triple-product correlations of outgoing and incoming proton momenta [7, 38].

Acknowledgments

The work was supported by the project LG13009 of the Ministry of Education of the Czech republic. The author wishes to thank Sven Heinemeyer and Valery Khoze who participated at the early stage of this analysis for their encouragement and assistance.

References

- [1] V.A. Khoze, A.D. Martin and M.G. Ryskin, Eur. Phys. J. **C 14** (2000) 525 [arXiv:hep-ph/0002072].
- [2] M. Albrow and A. Rostovtsev, arXiv:hep-ph/0009336.
- [3] V.A. Khoze, A.D. Martin and M.G. Ryskin, Eur. Phys. J. **C 23** (2002) 311 [arXiv:hep-ph/0111078].
- [4] For a review see M. Albrow, T. Coughlin and J. Forshaw Prog. Part. Nucl. Phys. **65** (2010) 149 [arXiv:1006.1289 [hep-ph]].
- [5] A. De Roeck, V.A. Khoze, A.D. Martin, R. Orava and M.G. Ryskin, Eur. Phys. J. **C 25** (2002) 391 [arXiv:hep-ph/0207042].
- [6] V.A. Khoze, A.D. Martin, M.G. Ryskin and A. Shuvaev, Eur. Phys. J. **C 68** (2010) 125 [arXiv:1002.2857 [hep-ph]].
- [7] L.A. Harland-Lang, V.A. Khoze, M.G. Ryskin and W.J. Stirling, arXiv:1301.2552 [hep-ph].
- [8] CMS and TOTEM diffractive and forward physics working group, CERN/LHCC 2006-039/G-124, CMS Note 2007/002, TOTEM Note 06-5, December 2006.
- [9] M. Albrow et al. (FP420 R&D Collab.), JINST **4** (2009) T10001 [arXiv:0806.0302 [hep-ex]].
- [10] The AFP project in ATLAS, Letter of Intent of the Phase-I Upgrade (ATLAS Collab.), <http://cdsweb.cern.ch/record/1402470>;
C. Royon, arXiv:1302.0623 [physics.ins-det];
M. Tasevsky, Nucl. Phys. Proc. Suppl. **179-180** (2008) 187.
- [11] The PPS upgrade project in CMS, M. Albrow, AIP Conf. Proc. **1523** (2012) 320.
- [12] C. Royon, AIP Conf. Proc. **1105** (2009) 130.
- [13] J. de Favereau de Jeneret et al., arXiv:0908.2020 [hep-ph].
- [14] P. Bussey, T. Coughlin, J. Forshaw and A. Pilkington, JHEP **0611** (2006) 027 [arXiv:hep-ph/0607264].
- [15] M. Tasevsky, arXiv:0910.5205 [hep-ph].

- [16] A. Kaidalov, V.A. Khoze, A.D. Martin and M.G. Ryskin, Eur. Phys. J. **C 33** (2004) 261 [arXiv:hep-ph/0311023].
- [17] S. Heinemeyer, V.A. Khoze, M.G. Ryskin, W.J. Stirling, M. Tasevsky and G. Weiglein, Eur. Phys. J. **C 53** (2008) 231 [arXiv:0708.3052 [hep-ph]].
- [18] S. Heinemeyer, V.A. Khoze, M.G. Ryskin, M. Tasevsky and G. Weiglein, Eur. Phys. J. **C 71** (2011) 1649 [arXiv:1012.5007 [hep-ph]].
- [19] B. Cox, F. Loebinger and A. Pilkington, JHEP **0710** (2007) 090 [arXiv:0709.3035 [hep-ph]].
- [20] J. Forshaw et al., JHEP **0804** (2008) 090 [arXiv:0712.3510 [hep-ph]].
- [21] S. Heinemeyer et al., arXiv:0811.4571 [hep-ph].
- [22] M. Chaichian, P. Hoyer, K. Huitu, V. A. Khoze and A. Pilkington, JHEP **0905** (2009) 011 [arXiv:0901.3746 [hep-ph]].
- [23] S. Heinemeyer, V.A. Khoze, M.G. Ryskin, M. Tasevsky and G. Weiglein, arXiv:0909.4665 [hep-ph]; arXiv:1009.2680 [hep-ph].
- [24] S. Heinemeyer, V.A. Khoze, M.G. Ryskin, M. Tasevsky and G. Weiglein, arXiv:1106.3450 [hep-ph];
- [25] J. Ellis, J. Lee and A. Pilaftsis, Phys. Rev. **D 71** (2005) 075007 [arXiv:hep-ph/0502251].
- [26] M. Carena, J. Ellis, A. Pilaftsis and C. Wagner, Phys. Lett. **B 495** (2000) 155 [hep-ph/0009212].
- [27] A. Djouadi, arXiv:1311.0720 [hep-ph];
- [28] M. Boonekamp, J. Cammin, S. Lavignac, R. Peschanski and C. Royon, Phys. Rev. **D 73** (2006) 115011 [arXiv:hep-ph/0506275].
- [29] A. Brandt, V. Juranek, A. Pal and M. Tasevsky, ATL-COM-PHYS-2010-337.
- [30] B.E. Cox et al., Eur. Phys. J. **C 45** 401 [hep-ph/0505240].
- [31] M. Tasevsky, AIP Conf. Proc. **828** (2006) 401.
- [32] V.A. Khoze, A.D. Martin and M.G. Ryskin, Eur. Phys. J. **C 19** (2001) 477 [Erratum-ibid. **C 20** (2001) 599] [arXiv:hep-ph/0011393].
- [33] A.B. Kaidalov, V.A. Khoze, A.D. Martin and M.G. Ryskin, Eur. Phys. J. **C 31** (2003) 387 [arXiv:hep-ph/0307064].
- [34] M. Dührssen, S. Heinemeyer, H. Logan, D. Rainwater, G. Weiglein and D. Zeppenfeld, Phys. Rev. **D 70** (2004) 113009 [arXiv:hep-ph/0406323]; [arXiv:hep-ph/0407190].
- [35] R. Lafaye, T. Plehn, M. Rauch, D. Zerwas and M. Dührssen, JHEP **0908** (2009) 009 [arXiv:0904.3866 [hep-ph]].

- [36] A. David et al. (LHC Higgs Cross Section Working Group), arXiv:1209.0040 [hep-ph].
- [37] S. Heinemeyer, C. Mariotti, G. Passarino and R. Tanaka (eds.) (LHC Higgs Cross Section Working Group), arXiv:1307.1347 [hep-ph].
- [38] V.A. Khoze, A.D. Martin and M.G. Ryskin, Eur. Phys. J. **C 34** (2004) 327 [arXiv:hep-ph/0401078].
- [39] H. Nilles, Phys. Rept. **110** (1984) 1.
- [40] H. Haber and G. Kane, Phys. Rept. **117** (1985) 75.
- [41] R. Barbieri, Riv. Nuovo Cim. **11** (1988) 1.
- [42] M. Carena and H. Haber, Prog. Part. Nucl. Phys. **50** (2003) 63 [arXiv:hep-ph/0208209].
- [43] S. Heinemeyer, Int. J. Mod. Phys. **A 21** (2006) 2659 [arXiv:hep-ph/0407244].
- [44] S. Heinemeyer, W. Hollik and G. Weiglein, Phys. Rept. **425** (2006) 265 [arXiv:hep-ph/0412214].
- [45] A. Djouadi, Phys. Rept. **457** (2008) 1 [arXiv:hep-ph/0503172]; Phys. Rept. **459** (2008) 1 [arXiv:hep-ph/0503173].
- [46] M. Carena, S. Heinemeyer, C. Wagner and G. Weiglein, Eur. Phys. J. **C 26** (2003) 601 [arXiv:hep-ph/0202167].
- [47] A. Shuvaev et al., Eur. Phys. J. **C 56**, 467 (2008) [arXiv:0806.1447 [hep-ph]].
- [48] V.A. Khoze, A.D. Martin and M.G. Ryskin, Eur. Phys. J. **C 64** (2009) 361 [arXiv:0907.0966 [hep-ph]].
- [49] S. Heinemeyer, W. Hollik and G. Weiglein, Comp. Phys. Commun. **124** (2000) 76 [arXiv:hep-ph/9812320].
- [50] T. Hahn, S. Heinemeyer, W. Hollik, H. Rzehak and G. Weiglein, Comp. Phys. Commun. **180** (2009) 1426; see: www.feynhiggs.de .
- [51] S. Heinemeyer, W. Hollik and G. Weiglein, Eur. Phys. J. **C 9** (1999) 343 [arXiv:hep-ph/9812472].
- [52] G. Degrandi, S. Heinemeyer, W. Hollik, P. Slavich and G. Weiglein, Eur. Phys. J. **C 28** (2003) 133 [arXiv:hep-ph/0212020].
- [53] M. Frank, T. Hahn, S. Heinemeyer, W. Hollik, H. Rzehak and G. Weiglein, JHEP **0702** (2007) 047 [arXiv:hep-ph/0611326].
- [54] P. Bechtle, O. Brein, S. Heinemeyer, G. Weiglein and K. Williams, Comput. Phys. Commun. **181** (2010) 138 [arXiv:0811.4169 [hep-ph]]; Comput. Phys. Commun. **182** (2011) 2605 [arXiv:1102.1898 [hep-ph]].

- [55] P. Bechtle, O. Brein, S. Heinemeyer, O. Stål, T. Stefaniak, G. Weiglein and K. Williams, arXiv:1301.2345 [hep-ph]; the code and manual can be obtained via www.ippp.dur.ac.uk/HiggsBounds.
- [56] J. Ellis, S. Heinemeyer, K. Olive, A. Weber, G. Weiglein, JHEP **0708** (2007) 083 [arXiv:0706.0652 [hep-ph]].
- [57] J. Ellis, T. Hahn, S. Heinemeyer, K. Olive and G. Weiglein, JHEP **0710** (2007) 092 [arXiv:0709.0098 [hep-ph]].
- [58] G. Kribs, T. Plehn, M. Spannowsky and T. Tait, Phys. Rev. D **76** (2007) 075016 [arXiv:0706.3718 [hep-ph]].
- [59] A. Djouadi and A. Lenz, Phys. Lett. B **715** (2012) 310 [arXiv:1204.1252 [hep-ph]].
- [60] G. Aad et al. (ATLAS Collab.), ATLAS-CONF-2013-034;
- [61] S. Chatrchyan et al. (CMS Collab.), CMS-PAS-HIG-13-005.
- [62] G. Aad et al. (ATLAS Collab.), Phys. Lett. B **718** (2013) 1284 [arXiv:1210.5468[hep-ex]].
- [63] S. Chatrchyan et al. (CMS Collab.), Phys. Lett. B **718** (2012) 307 [arXiv:1209.0471 [hep-ex]].
- [64] T. Aaltonen et al. (CDF and D0 Collab.), arXiv:1303.6346 [hep-ex], submitted to Phys. Rev. D.
- [65] G. Aad et al. (ATLAS Collab.), Phys. Lett. B **716** (2012) 1.
- [66] S. Chatrchyan et al. (CMS Collab.), Phys. Lett. B **716** (2012) 30.
- [67] G. Aad et al. (ATLAS Collab.), arXiv:1307.1432 [hep-ex], submitted to Phys. Lett. B; ATLAS-CONF-2013-040.
- [68] S. Chatrchyan et al. (CMS Collab.), Phys. Rev. Lett. **110** (2013) 081803 [arXiv:1212.6639 [hep-ex]]; CMS-PAS-HIG-13-002.
- [69] G. Aad et al. (ATLAS Collab.), arXiv:1307.1427 [hep-ex], submitted to Phys. Lett. B.
- [70] S. Chatrchyan et al. (CMS Collab.), CMS-PAS-HIG-13-005.
- [71] M. Carena, S. Heinemeyer, O. Stål, C.E.M. Wagner and G. Weiglein, arXiv:1302.7033 [hep-ph].
- [72] A. Martin, M. Ryskin and G. Watt, Eur. Phys. J. C **66** (2010) 163 [arXiv:0909.5529 [hep-ph]].
- [73] T. Coughlin and J. Forshaw, JHEP **1001** (2010) 121 [arXiv:0912.3280 [hep-ph]].
- [74] V.A. Khoze, A.D. Martin and M.G. Ryskin, Phys. Lett. B **650** (2007) 41 [arXiv:hep-ph/0702213].

- [75] V.A. Khoze, M.G. Ryskin and W.J. Stirling, Eur. Phys. J. **C 48** (2006) 477 [arXiv:hep-ph/0607134].
- [76] R. Maciula, A. Szczurek and R. Pasechnik, Phys. Rev. **D 83** (2011) 114034 [arXiv:1011.5842 [hep-ph]].
- [77] A.D. Martin, M.G. Ryskin and V.A. Khoze, Acta Phys. Polon. **B 40** (2009) 1841 [arXiv:0903.2980 [hep-ph]].
- [78] M.G. Ryskin, A.D. Martin and V.A. Khoze, Eur. Phys. J. **C 60** (2009) 265 [arXiv:0812.2413 [hep-ph]].
- [79] L.A. Harland-Lang, V.A. Khoze, M.G. Ryskin and W.J. Stirling, Eur. Phys. J. **C72** (2012) 2110 [arXiv:1204.4803 [hep-ph]].
- [80] L.A. Harland-Lang, V.A. Khoze, M.G. Ryskin and W. J. Stirling, Eur. Phys. J. **C 69** (2010) 179 [arXiv:1005.0695 [hep-ph]].
- [81] J. Pumplin et al., JHEP **0207** (2002) 012 [arXiv:0201.195 [hep-ph]].
- [82] T. Aaltonen et al. (CDF Collab.), Phys. Rev. Lett **108** (2012) 081801 [arXiv:0707.2374 [hep-ex]].
- [83] V.A. Khoze, A.D. Martin and M.D. Ryskin, Eur. Phys. J. **C 55** (2008) 363 [arXiv:0802.0177 [hep-ph]].
- [84] L. Bonnet, T. Pierzchala, K. Piotrkowski and P. Rodeghiero, Acta Phys. Polon. **B 38** (2007) 477 [arXiv:hep-ph/0703320].
- [85] K. Piotrkowski and N. Schul, AIP Conf. Proc. **1200** (2010) 434 [arXiv:0910.0202 [hep-ph]].
- [86] G. Aad et al. (ATLAS Collab.), ATLAS-CONF-2011-089.
- [87] S. Chatrchyan et al. (CMS Collab.), J. Inst. **8** (2013) P04013.
- [88] M. Carena, S. Heinemeyer, C. Wagner and G. Weiglein, Eur. Phys. J. **C 45** (2006) 797 [arXiv:hep-ph/0511023].
- [89] S. Schael et al. (ALEPH, DELPHI, L3, OPAL Collaborations and LEP Working Group for Higgs boson searches), Eur. Phys. J. **C 47** (2006) 547 [arXiv:hep-ex/0602042].
- [90] See the latest results at <http://tevnpnphwg.fnal.gov> (New Phenomena and Higgs Working Group):
Tevatron New Phenomena and Higgs Working Group, arXiv:1003.3363 [hep-ex];
T. Aaltonen et al. (CDF and D0 Collaborations), Phys. Rev. **D 86** 091101 [arXiv:1207.2757 [hep-ex]];
T. Aaltonen et al. (CDF Collaboration), Phys. Rev. Lett. **103** (2009) 101803 [arXiv:0907.1269 [hep-ex]]; Phys. Rev. **D 85** (2012) 032005 [arXiv:1106.4782 [hep-ex]];

- V. M. Abazov et al. (D0 Collab.), Phys. Lett. **B 698** (2011) 97 [arXiv:1011.1931 [hep-ex]]; Phys. Lett. **107** (2011) 121801 [arXiv:1106.4885 [hep-ex]]; Phys. Lett. **B 710** (2012) 569 [arXiv:1112.5431 [hep-ex]]; Phys. Lett. **B 698** (2011) 97 [arXiv:1011.1931 [hep-ex]];
- [91] S. Lai, EPJ Web Conf. **49** (2013) 09005 [arXiv:1303.4064 [hep-ex]].
- [92] B. Petersen, cds.cern.ch/record/14951472?ln=en.
- [93] G. Aad et al. (ATLAS Collab.), ATLAS-CONF-2013-090.
- [94] G. Abbiendi et al. (ALEPH, DELPHI, L3, OPAL Collaborations and LEP Working Group for Higgs boson searches), Phys. Lett. **B 565** (2003) 61 [arXiv:hep-ex/0306033].
- [95] R Harlander and W. Kilgore, Phys. Rev. **D 68** (2003) 013001 [arXiv:hep-ph/0304035].
- [96] A.D. Martin, R. Roberts, W.J. Stirling and R. Thorne, Eur. Phys. J. **C 28** (2003) 455 [arXiv:hep-ph/0211080].
- [97] A.D. Martin, W.J. Stirling, R. Thorne and G. Watt, Eur. Phys. J. **C 63** (2009) 189 [arXiv:0901.0002 [hep-ph]].
- [98] J. Butterworth, A. Davison, M. Rubin and G. Salam, Phys. Rev. Lett. **100** (2008) 242001 [arXiv:0802.2470 [hep-ph]].
- [99] G. Aad et al. (ATLAS Collab.), ATLAS-CONF-2013-079.
- [100] S. Chatrchyan et al. (CMS Collab.), CMS-PAS-HIG-13-012.
- [101] A. De Roeck et al., Eur. Phys. J. **C 66** (2010) 525 [arXiv:0909.3240 [hep-ph]].
- [102] S. Heinemeyer, V.A. Khoze, M. Tasevsky and G. Weiglein, arXiv:1206.0183 [hep-ph].
- [103] G. J. A. Brown et al., ATL-DAQ-PUB-2009-006, ATL-COM-DAQ-2009-062.